ANL/FPP/TM-296

PHYSICS OF COLLISIONLESS SCRAPE-OFF-LAYER PLASMA DURING NORMAL AND OFF-NORMAL TOKAMAK OPERATING CONDITIONS

by

Ahmed Hassanein

Isak Konkashbaev

March 1999

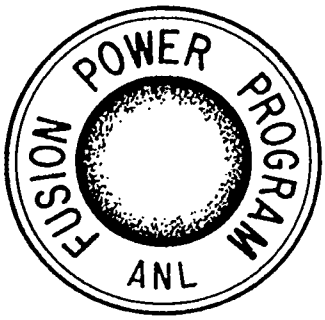

FUSION POWER PROGRAM

Argonne National Laboratory
9700 South Cass Avenue
Argonne, Illinois 60439

Operated by
The University of Chicago
for the U.S. Department of Energy
under Contract W-31-109-Eng-38

Reproduced from the best available copy.

Available to DOE and DOE contractors from the
Office of Scientific and Technical Information
P.O. Box 62
Oak Ridge, TN 37831
Prices available from (423) 576-8401

Available to the public from the
National Technical Information Service
U.S. Department of Commerce
5285 Port Royal Road
Springfield, VA 22161

Distribution Category:
Magnetic Fusion Reactor Materials

ANL/FPP/TM-296

ARGONNE NATIONAL LABORATORY
9700 South Cass Avenue
Argonne, Illinois 60439

Physics of Collisionless Scrape-Off-Layer Plasma during Normal and Off-Normal Tokamak Operating Conditions

by

Ahmed Hassanein
Fusion Power Program
Energy Technology Division
Argonne National Laboratory

Isak Konkashbaev
Troitsk Institute for Innovation and Fusion Research, Troitsk, Russia

March 1999

Work supported by the
Office of Fusion Energy
U.S. Department of Energy
Under Contract W-31-109-Eng-38

DISCLAIMER

Portions of this document may be illegible in electronic image products. Images are produced from the best available original document.

Physics of Collisionless Scrape-Off-Layer Plasma during Normal and Off-Normal Tokamak Operating Conditions

A. Hassanein* and I. K. Konkashbaev**

*Argonne National Laboratory, Argonne, IL, 60439, USA

**Troitsk Institute for Innovation and Fusion Research, Troitsk, Russia

Abstract

The structure of a collisionless scrape-off-layer (SOL) plasma in tokamak reactors is being studied to define the electron distribution function and the corresponding sheath potential between the divertor plate and the edge plasma. The collisionless model is shown to be valid during the thermal phase of a plasma disruption, as well as during the newly desired low-recycling normal phase of operation with low-density, high-temperature, edge plasma conditions.

An analytical solution is developed by solving the Fokker-Planck equation for electron distribution and balance in the SOL. The solution is in good agreement with numerical studies using Monte-Carlo methods. The analytical solutions provide an insight to the role of different physical and geometrical processes in a collisionless SOL during disruptions and during the enhanced phase of normal operation over a wide range of parameters.

I. Introduction

The steady operation of a plasma device is largely determined by the boundary conditions at the divertor or the limiter plates. The plasma processes at these boundary walls are complex and usually require extensive numerical simulation codes to obtain an insight into the relative importance of the different interaction phenomena and the desired optimal conditions for enhanced operations. The divertor plate, for example, in future fusion power machine is a key component in removing particle and heat fluxes. In conventional divertor operation of existing tokamaks, as well as in ITER-like device [1], the plasma in the scrape-off layer (SOL) is highly collisional ($T \approx 100$ eV), i.e., the particle mean free path, λ, is much shorter than the parallel or longitudinal distance, L, of the SOL between the two opposite (inner and outer) divertor plates. During normal operation of these devices, power to the divertor plates usually does not exceed the critical values at which melting or sublimation can occur. However, during plasma instabilities such as hard disruptions, edge-localized modes (ELMs), and vertical displacement events (VDEs), the high incident power, W_d, from the SOL ($W_d \geq 10^7$ W/cm^2) will cause significant erosion of the divertor plate and nearby components from surface vaporization, melt-layer splashing, and possible brittle destruction of carbon-based materials (CBMs) [2]. Although the actual heat flux arriving at the divertor plate during these events is significantly reduced due to the self-shielding effect from the divertor's own eroded material, the net erosion depth can still exceed hundreds of micrometers per event, which would lead to serious lifetime issues for these components [3]. From such numerical simulations and modeling experiments, the erosion lifetime

of the divertor plate material has been found to depend on both the magnitude of the incident heat flux from the SOL and the energy distribution of ion/electron fluxes to the divertor plate. Therefore, for more accurate predictions of plasma instability effects and for better-designed laboratory simulation experiments, a good knowledge of SOL physics and parameters is strongly needed.

During various plasma instability events, the loss of confinement will cause the majority of the core particle-flux, to arrive at the SOL with a relatively high temperature, $T \approx T_o$ where T_o (20-30 keV) is the core plasma temperature. This is in contrast to the normal operation scenario in which the escaping particles from the core plasma to the SOL have a relatively lower temperature, $T \leq 1$ keV and the plasma is collisional. Because of the high temperature of the escaping particles during plasma instability events, the SOL plasma becomes collisionless and requires different treatment than that of SOL behavior during normal operation [4].

Collisionless SOL plasma behavior is also encountered during the normal phase of operation with enhanced confinement [5,6]. This plasma operation with low particle recycling and high temperature near the divertor plate was demonstrated during recent device discharges of the JT-60U with the use of a boron-coated walls [7]. The plasma temperature in the SOL can be several keV, which will result in a collisionless plasma condition. The collisionless behavior of SOL during similar normal operations of large helical fusion devices with enhanced particle confinement was recently studied by numerical simulation with Monte Carlo methods [8].

We should emphasize that the term "collisionless" used in this report does not mean that collisions can always be neglected. The term is used only to indicate that the particle path length is much greater than the length of the SOL, i.e., the distance between the two opposite divertor plates along magnetic field lines. The full solution of the particle kinetic equation is still required, however, to describe particle distribution functions in the SOL. This is because particles that oscillate between plates located at distances much shorter than particle path length (collisionless in space) will have lifetimes determined by collisions (collisional in time). Similar situations exist in other plasma systems such as open magnetic traps and trapped particles in toroidal systems.

One of the main features of the collisionless SOL plasma is that the edge plasma acts as an electrostatic trap for electrons, since electrons which originally have parallel energy that is lower than the wall potential energy will be trapped between the inner and outer divertor plates. In a collisional SOL, however, because of the short path length of both ions and electrons, neutralization of the ion charge is due mainly to the SOL electrons moving toward the divertor plate. Therefore, in contrast to the collisional SOL, charge neutralization of ions in collisionless SOL plasma (see above definition) occurs mainly due to these trapped electrons. In more recent analyses, collisionless SOL plasma was studied (see, for example, Ref. 9) but without taking into account trapped particles oscillating between the two negatively charged inner and outer divertor plates. In this case, the full kinetic equation was not required. However, as will be shown below, the existence of trapped particles is very important and requires the full solution of the kinetic equation of particle transport, which will result in different SOL major parameters such as

negative potential and net heat load to divertor plates. More details on the origin and dynamics of trapped electrons can be found in Ref. 8.

II. Model Description of Collisionless SOL plasma

The electrons in the SOL are considered to be composed of three different populations based on their origins. Hot electrons arriving from the tokamak core plasma will have two different destinies according to their energy E and momentum $\vec{p}$. Electrons with parallel energy, $E_{||}$, and momentum, $P_{||} = mv_{||}$, along magnetic field lines that exceed the stopping potential, $|\phi|$, i.e., $E_{||} = p_{||}^2/2m > |\phi|$, will escape the SOL in the characteristic time $\tau_{||}^{hot} \approx L/V_{Te}$, where L is the average length of the open magnetic field lines in the parallel direction between the two opposite (inner and outer) divertor plates, and V_{Tc} is the thermal velocity of electrons $\left(V_{Te} = \sqrt{2T_o/m}\right)$. Such a flux of electrons, S_e^I, is referred to as the primary escaping electron flux.

The remaining flux of electrons with $P_{||}^2/2m < |\phi|$ will be trapped in the established electrostatic potential between the two opposite divertor plates. The characteristic lifetime of these trapped electrons is determined from the diffusion time in momentum space according to their collision frequencies. Because the lifetime of the trapped electrons is determined mainly by electron Coulomb collisions, these electrons can be considered as collisionless in space but collisional in time. If these electrons reach an energy, $E_{||} = p_{||}^2/2m > |\phi|$, due to collisions, these particles will then escape the SOL. This process is similar to the diffusion in the "cone of losses"

in the mirror trap devices. The flux of escaping electrons is referred to as the secondary escaping electron flux.

The third electron population in the SOL is that of the so-called "cold" electrons, which arrive from the divertor plates. This cold electron flux emitted from one wall (divertor plate) will pass through the SOL and be absorbed by the opposite wall. Therefore, the net current of the cold electrons is equal to zero (in a symmetrical SOL) since a similar value of cold electrons flux is emitted in the opposite direction by the other divertor plate. Residence time of these cold electrons in the SOL can be estimated by $\tau_{ll}^{cold} \approx L/V_c$, where $V_c = \sqrt{2e\phi/m}$, which is similar to V_{Tc} since $e\varphi \approx KT_0$; therefore their residence time is also much less than the electron collision time and such electrons can also be regarded as fully collisionless. A schematic illustration of the various electron populations in a collisionless SOL plasma is shown in Fig. 1.

Because the potential, ϕ, changes rapidly only in a very small region near the divertor plates (walls) with width $\Delta L \ll L$ (as shown schematically in Fig. 2), a simple one-dimensional representation of the potential function can be given by:

$$\begin{aligned} \phi(x) &= -\phi_o \qquad x = 0, L \\ \phi(x) &= 0 \qquad 0 < x < L. \end{aligned} \tag{2-1}$$

This means that the SOL plasma can be regarded as a homogeneous plasma region along the magnetic field lines. In this study, we also assume that the SOL plasma is homogeneous across the magnetic field lines. Nonhomogeneous effects in the SOL plasma will be considered in a followup study.

The trapped electrons in the SOL, i.e., with $E_{\parallel} < e\phi_o$, will move between the two opposite divertor plates with a bouncing frequency, f_E, given by

$$f_E = \frac{V_{Te}}{L}. \tag{2-2}$$

Different electron bouncing frequencies will result in "phase-mixing" of the electrons and therefore the distribution of these electrons can be considered as homogeneous in space. Due to Coulomb collisions, the electron diffusion takes place along the $V_{\parallel}$ axis in the momentum space. The lifetime of these trapped electrons, τ_e^{trap}, to escape the SOL can be estimated by $\tau_e^{trap} \approx \tau_{ee}$, where τ_{cc} is the electron/electron Coulomb collision time. The escaping electron flux due to these collisions is referred to as the secondary escaping electron flux, S_e^{II}. The third electron population in the SOL, i.e., the "cold" or "secondary" electrons is emitted by the wall such that:

$$j_e^{hot} + j_e^{cold} + j_e^{trap} + j_i = 0, \tag{2-3}$$

where j_e^{hot} is the escaped electron current, j_e^{cold} is the cold (secondary) electron current, j_e^{trap} is the trapped electron current, and j_i is the ion current to the wall.

The cold electron current $j_e^{cold} = eS_e^{cold}$, where S_e^{cold} is the emitted cold electron flux from the walls. This cold electron flux emitted by one wall (divertor plate) will pass through the SOL and be absorbed by the opposite wall. Therefore, for a symmetrical SOL the net current of the cold electrons is equal to zero since a similar value in the opposite direction of cold electorn flux is emitted by the other divertor plate, i.e., $j_e^{cold} = 0$. In general, however, not all the emitted electrons will reach the other divertor plate due to collisional trapping during their flight along the SOL. The residence time of the cold electron flux, τ_e^{cold}, can be estimated by

$$\tau_e^{cold} \approx \frac{L}{\sqrt{2e\phi_o/m}}. \tag{2-4}$$

This residence time is, however, about three orders of magnitude lower than the electron collision time. Therefore, collisions of cold electrons as well as that of the escaping hot electrons with both the trapped electrons and ions can be neglected. The emitted electron flux, S_{out}^I, due to the primary escaping hot electron flux, will depend on the wall potential, ϕ_o, and the wall emissivity, γ, such that $S_{out}^I = \gamma S_e^I$.

The ion current, j_i, in the SOL is equal to the ion current arriving from the core plasma. The average ion velocity $V_{\parallel}^{i}$ in the SOL is approximately similar to that of the thermal ion velocity V_{Ti}:

$$V_{\parallel}^{i} \approx V_{Ti} = \sqrt{2T_o/M}, \tag{2-5}$$

where M is the average ion mass. The residence time of these ions in the SOL is given by

$$\tau_{\parallel}^{i} = \frac{L}{V_{\parallel}^{i}} \approx \sqrt{M/m}\,\tau_{\parallel}^{hot}, \tag{2-6}$$

where $\tau_{\parallel}^{hot}$ is again the characteristic time of the escaping hot electrons in the SOL.

Near the wall where the potential is sharply decreased from 0 to ϕ_o, the ions are accelerated to a velocity given by

$$V_{wall}^{i} \approx \sqrt{\frac{2e\phi}{M} + \left(V_{\parallel}^{i}\right)^2}. \tag{2-7}$$

However, within the developed model of a homogeneous SOL plasma, one can neglect this acceleration because it will not significantly influence the main results, as will be shown later.

During normal operation, as well as during disruptions, two types of heat fluxes arrive at the SOL from the core plasma: particle heat flux, W_p, carried by the lost particle fluxes of both electrons (S_e) and ions (S_i) and heat flux, W_k, due to heat diffusion. The particle fluxes $S_{e,i}$ usually have an ambipolar nature; therefore:

$$S_e = S_i = S_{in}, \tag{2-8}$$

The value of S_{in} can be estimated as

$$S_{in} = \frac{n_o \cdot 2\pi R \cdot \pi r^2}{\tau_p}, \tag{2-9}$$

where R is the major radius, r is the minor radius, n_o is core plasma density, and τ_p is the particle confinement time. The corresponding particle heat flux is $W_p = 3KT_0 S_{in}$. The conduction heat flux, W_k, is estimated as

$$W_k = \frac{Q_o}{\tau_k}, \text{ and } Q_o = n_o.3KT.2\pi R.\pi r^2, \tag{2-10}$$

where τ_k is the characteristic time of heat loss due to conduction and K is Boltzmann's constant. The total heat flux W_0 arriving at the SOL can therefore be estimated as

$$W_0 = \frac{Q_o}{\tau_E}\ , \text{ and } \frac{1}{\tau_E} = \frac{1}{\tau_k} + \frac{1}{\tau_p}\ , \tag{2-11}$$

where τ_E is the energy confinement time. The relationship between W_k and W_p is given by

$$\eta = \frac{\tau_p}{\tau_k}. \tag{2-12}$$

For normal operation, usually

$$\tau_k < \tau_p \text{ , and therefore } \eta > 1. \tag{2-13}$$

During a tokamak disruption, however, the situation is not so clear. From the experiments carried out in the JET device [10] the core plasma density, n_0, decreased during disruption slower than the decrease in electron temperature , T_{e0}. Recent experiments performed in the TFTR machine [11] have indicated that the ion temperature, T_{i0}, obtained from a neutron signal also decreased slower than T_{e0}. One can conclude that the turbulent heat conduction flux, W_k, may play an important role compared to particle loss, i.e., $\tau_k \neq \infty$, and $\eta \neq 0$. There are no separate measurements of heat flux losses due to the heat conduction or the heat flux carried by the lost particles. The total energy flux lost, W_0, is usually estimated by dividing the total core plasma energy, Q_0, over the disruption time τ_d. Because of the lack of separate measurements of W_k and W_p it is asumed in this analysis that $W_p = W_d$ and $W_k = 0$, $\eta = 0$. In future work it is possible to separate W_0 into both W_p and W_k , and then it will be feasible to take into account the

effect of heat conduction. In section V it will be shown how both W_p and W_k can be considered separately.

The ion density, n_i, in the SOL can be estimated from the stationary condition that $S_{II}^{i} = S_{in}$, where the ion flux, S_{II}^{i}, from the SOL to the divertor plate is given by

$$S_{II}^{i} = \frac{1}{\sqrt{2\pi}} V_{Ti} n_i 2\pi r h \frac{1}{q_s}, \text{ and } q_s = \frac{L}{2\pi R} \approx \frac{RB_\varphi}{rB_\vartheta}, \tag{2-14}$$

where h is the SOL width, B_φ, *and* B_θ are the mean values of the poloidal and toroidal magnetic fields in the SOL respectively. The q_s value depends on the specific tokamak geometry and is usually close to unity in the SOL and is assumed equal to 1 in this analysis. Therefore n_i is given by

$$n_i = \frac{\sqrt{2\pi^3}\,\mathrm{Rr}}{V_{Ti}\, h\, \tau_p} n_0. \tag{2-15}$$

The total electron density in the SOL is the sum of all densities of the three different electron populations defined above. The total flux of the cold electrons, S_e^{cold}, is defined by

$$S_e^{cold} = S_{out}^{I} + S_{out}^{II} = \gamma\left(S_e^{I} + S_e^{II}\right), \tag{2-16}$$

where γ is again the wall emissivity of the secondary electrons.

The condition of quasineutrality of the SOL plasma is given by

$$n_i = n_e = n_e^{I,II} + n_e^{trap} + n_e^{cold}, \tag{2-17}$$

where $n_e^{I,II}$ are the densities of the primary and secondary escaping electrons, respectively, n_e^{trap} is density of the trapped electrons, and n_e^{cold} is the density of the cold electrons.

In a collisionless SOL, the trapped electron density is much higher than in a collisional SOL plasma due to the very low density of both the escaping and cold electron populations in the collisionless layer. For typical parameters of V_{Te} (10 keV) $\approx 6 \times 10^9$ cm/s, R ~ 10 m, r ~ 1 m, and h $\approx$ 3 cm, the escaping-electron density is

$$n_e^{I,II} \approx \frac{S_e^{I,II}}{V_{Te} 2\pi r h} = n_0 \frac{\pi R r}{V_{Te} h \tau_p} << n_0 . \tag{2-18}$$

For the same reason, the resulting cold electron density is also low. Therefore, the positive ion charge is neutralized mainly by the negative charge of the trapped electrons, and

$$n_i \approx n_e^{trap}. \tag{2-19}$$

The main problem is thus to find the value of the trapped electron density, n_e^{trap}.

III. Analytical Solution

The problem now consists of solving the stationary state of the trapped electron population density in the SOL plasma. An equilibrium electron density is established between the incoming flux of electrons from the core plasma and the outgoing escaping electron flux. The incoming electron flux arrives at the trap in the SOL from the core by crossing the separatrix between the open and the closed magnetic field lines and then escapes by crossing the separatrix between the trapped and escaping electrons (in momentum space).

The kinetic equation for the electron distribution function, F, is given by the Fokker-Planck equation [12]:

$$\frac{\partial F}{\partial t} + \bar{\upsilon}_\alpha \frac{\partial F}{\partial X_\alpha} + \frac{\partial}{\partial P_\alpha}\left(\bar{G}_\alpha \cdot F\right) + \frac{\partial I_\alpha}{\partial P_\alpha} = q\left(\vec{x}, \vec{P}\right), \tag{3-1}$$

where $\bar{G}_\alpha$ is the electromagnetic force, P_α is momentum in direction $\vec{x}_\alpha$, I_α is diffusion flux in momentum space, q is a source and loss term, and α is the coordinate frame (x, y, z) or (ϕ, θ, Z). For a stationary solution, $\frac{\partial F}{\partial t} = 0$, and for a homogenous distribution in SOL, $\upsilon_\alpha \frac{\partial F}{\partial P_\alpha} = 0$. The

electric field effect is taken into account at the boundary conditions. The magnetic field does not affect the distribution function F. The vector I in Eq. 3-1 specifies the electron density flux in momentum space arising from particle collisions. It is defined by

$$I_\alpha = A_\alpha F - D_{\alpha\beta} \frac{\partial F}{\partial P_\beta}, \tag{3-2}$$

where the vector $\bar{A}$ is the of dynamic friction coefficient and the tensor $D_{\alpha\beta}$ is the particle diffusion coefficient in momentum space.

Figure 3 is a schematic illustration of the trapped-particle zones in momentum space. Three regions are shown for different trapped particles in momentum space. Region I is occupied with trapped particles having total energy less than that required to overcome the electrostatic barrier at the walls. Region II is filled with particles having $P > P^* \left(P^* = m\upsilon^* = \sqrt{2me\phi_o}\right)$. Only scattering without energy exchange is sufficient for the particles to escape this region. Region III contains very low densities of escaping and cold electrons. One of the objectives of this work is to find an analytical solution to easily study the dependence of the solution on device characteristics (both physical and geometrical) in order to understand the significance and effect of each parameter on the SOL characteristics. The analytical solution can, however, be obtained using few assumptions. The validity and justification of these assumptions will be critically assessed as we proceed to find the analytical solution.

The first assumption is that one can neglect the influence of particles in region II (Fig. 3). This can be justified for several reasons. First, particles in region II can easily escape due to scattering by both ions and electrons because these particles need only a change in their angular momentum during a time $t \approx \tau_{ee} \approx \tau_{ei}$. Such elastic collision processes are much faster than particle diffusion along the P-axis with increasing total momentum due only to electron scattering. Another reason for neglecting the influence of particles in region II is because particles in this region are in the nonequilibrium state because $\langle P_{\parallel} \rangle \neq \langle P_{\perp} \rangle$. For situations in which parallel particle momentum does not equal perpendicular momentum, a "fire-hose" Alven wave instability usually takes place with a maximum increment on the order of the ion gyrofrequency, ω_{Bi}, which is much greater than the characteristic time, τ_c, [13], i.e,

$$\omega_{Bi} \approx 10^8 \text{ Hz} >> \frac{1}{\tau_e} \approx 10^3 \text{ Hz}. \tag{3-3}$$

The resulting turbulence effect of this instability is to equalize $\langle P_{\parallel} \rangle$ and $\langle P_{\perp} \rangle$. In this case, it means that additional transverse momentum, $\langle P_{\perp} \rangle$, is transferred to parallel momentum, $\langle P_{\parallel} \rangle$. Therefore, particles in region II with their parallel momentum $\langle P_{\parallel} > P^* \rangle$ will escape. More detailed description of the relaxation of such anisotropic distribution for homogeneous media is given in [14].

By neglecting the contribution of particles in region II, we can reduce the problem to a more simple one of particle diffusion in region I along the axis P (see Fig. 4). Therefore, the trapped-electron distribution function, F, is similar to that of the schematic illustration shown in Fig. 5. The function F, for the reduced problem, does not depend on the angle θ, i.e., F is an isotropic function. Therefore, Equation 3-1 is reduced to

$$\frac{1}{P^2}\frac{\partial}{\partial P}\left[P^2\left(D\ \frac{\partial F}{\partial P}-AF\right)\right]=-q(P), \tag{3-4}$$

where the source function, q, (per unit volume of phase space per second), the diffusion coefficient, D, and the dynamic friction, A, are also isotropic functions of P.

An exact solution of this problem is still difficult since the coefficients D of diffusion and A of the dynamical friction are unknown but are needed for the solution to the distribution function F. This means that the problem is highly nonlinear. Computer methods such as Monte-Carlo can be used to solve this problem numerically [8]. However to obtain an analytical solution, some arbitrary assumptions must be made. It will be evident, however, from the developed solution that the basic features of the phenomenon will be not lost due to these assumptions. A similar problem to estimate electron losses from open mirror traps was obtained in the case of a large wall potential, $|e\varphi/kT| \gg 1$ [15].

To obtain an analytical solution for the distribution function in the case considered, one can use the diffusion approximation in which D and A are replaced by a known function of P. If we allow both D and A to be represented by an expression for a Maxwellian velocity distribution, then seek the function, F, in the form

$$F = \frac{1}{(2\pi)^{3/2}} C_q \cdot f(P)\, e^{-p^2/2}, \tag{3-5}$$

where C_q is a constant that includes parameters from the source function q(P). Hereafter the dimensionless momentum, P, and the dimensionless potential, Ψ, are defined as

$$P = mV / P_o \ , \ P_o = \sqrt{KT_o.m} \ , \text{and} \ \ \psi = e\varphi_o / KT_o \tag{3-6}$$

The diffusion mechanism of particle losses results in a rather weak dependence of the normalized wall potential, ψ^*, and the corresponding momentum, $P^* = \sqrt{2\psi^*}$, on tokamak parameters since these effects are integrated over the velocity space which tends to average the detailed structure of the function F. Therefore, the obtained analytical solution is considered a good approximation to this problem. To calculate D and A, the function f(P) in Eq. 3-5 will be assumed equal to 1, therefore D and A are given by

$$D = \nu(P), \quad A = -\nu(P) \cdot P, \tag{3-7}$$

where ν (P) is the dependence of the collisional frequency on P,

$$\nu(P)=\frac{4\pi\lambda n_e^{trap}}{m^2V^3}=\nu_o(T_o)\frac{n_e^{trap}}{n_o}\frac{1}{P^3} \tag{3-8}$$

in which the unknown density, n_e^{trap}, of the trapped electrons will be found from the solution. The use of such assumption makes possible to find an analytical solution for this problem.

The source function q(P) is the electron distribution function arriving from the core plasma. Therefore, q(P) is taken to be a Maxwellian distribution. Finally, the dimensionless equation for the electron distribution function F can be rewritten as

$$\frac{1}{P^2}\frac{\partial}{\partial P}\left[\frac{1}{P}\left(\frac{\partial F}{\partial P}+PF\right)\right]=-a\,q(P),$$

$$q(P)=\frac{1}{(2\pi)^{3/2}}e^{-P^2/2}, \tag{3-9}$$

The parameter a includes parameters of the tokamak device

$$a=\frac{r}{2h}\frac{1}{\nu_0\tau_p}\left(\frac{n_0}{n_e^{trap}}\right)^2\frac{1}{C_q}\ . \tag{3-10}$$

This form of equation has a solution in the form

$$F=\frac{1}{(2\pi)^{3/2}}C_q e^{-p^2/2}\left[1-aP+a\frac{P^3}{3}+a\frac{\sqrt{2\pi}}{2}e^{p^2/2}\ \phi(P)\right] \tag{3-11}$$

where

$\phi(P)=\frac{2}{\sqrt{2\pi}}\int_0^P e^{-\xi^2/2}\,d\xi$ is the probability integral.

The constant C_q is defined from the normalization condition

$$4\pi\int F(P)P^2\,dP=n_e^{trap}\ , \tag{3-12}$$

where n_e^{trap} = n_i according to Eq. 2-19. The value of P^* can be found from the boundary condition $F(P^*) = 0$. The solution of this boundary equation and the dependence of the normalized wall potential, ψ^*, on the parameter, a, is found numerically, as shown in Fig.7. The solution, however, has the following two asymptotes:

$$a\to\infty;\ P^*\Rightarrow\left(\frac{3.5}{a}\right)^{1/5}\text{ and }\psi^*\Rightarrow\frac{1}{2}\left(\frac{3\cdot5}{a}\right)^{2/5} \tag{3-13}$$

$$a\to 0;\ P^*\Rightarrow\sqrt{2\ln\left(\frac{2}{\sqrt{2\pi}}\frac{1}{a}\right)}\text{ and }\psi^*\Rightarrow\ln\left(\frac{2}{\sqrt{2\pi}}\frac{1}{a}\right). \tag{3-14}$$

The parameter, a, defined from C_q is also calculated numerically with the asymptotes:

$$P^*\to\infty;\ a\Rightarrow\frac{1}{4\pi}\frac{\tau_p V_{To}^2 h}{\nu_o R^2 r} \tag{3-15}$$

$$P^* \to 0;\ a \Rightarrow \frac{(15)^{6/11}}{(2\pi^2)^{5/11}} \left(\frac{\tau_p V_{To}^2 h}{\nu_o R^2 r} \right)^{5/11} . \qquad (3\text{-}16)$$

Thus the wall potential, ϕ_o, depends on tokamak dimensions (i.e., R, r), on plasma density and temperature via electron collision frequency, ν_o, on the thermal velocity of ions, V_{Ti}, and on the particle confinement time, τ_p.

IV. Disruption Conditions

For future tokamak devices with major radius $R \approx 6$ m, minor radius $r \approx 1$ m, plasma core temperature $T_o \approx 20$ keV, and core density $n_o = 10^{14}$ cm^{-3}, the disruption time, τ_d, is $\approx$1 ms. The parameter, a, for such a device is calculated to be large, $a \approx 20$. This means that we can use the asymptotic solutions given in Eq. 3-13 to estimate the wall potential. Therefore,

$$P^* \approx 0.9 \text{ and } \psi^* \approx 0.5 . \qquad (4\text{-}1)$$

The density of the trapped electrons is therefore estimated as

$$n_e^{trap} \approx 3 n_0 . \qquad (4\text{-}2)$$

The fraction, ξ, of the incoming electrons that is trapped in the SOL is given by

$$\xi = \frac{\int_0^{P^*} e^{-P^2/2}\, P^2\, dp}{\int_0^{\infty} e^{-P^2/2}\, P^2 dp} \approx 0.3. \qquad (4\text{-}3)$$

The temperature (mean energy), T_e^{trap}, of the trapped electrons in the SOL having the non-Maxwellian distribution function of Eq. 3-9 is lower than the core temperature T_o:

$$T_e^{trap} = T_{SOL} < \psi^* T_0 \approx 9\ keV\ . \qquad (4\text{-}4)$$

The assumption of F (P=P*)= 0 means that all electrons leaving the trap will have P = P*, which means that their energy at the wall, E_t^W, after overcoming the stopping potential, ϕ_o, is equal to zero; i.e.,

$$E_t^W = 0\ . \qquad (4\text{-}5)$$

In reality, however, the distribution function, F, has a sharp "tail" at P > P*; therefore, electrons diffusing from the trap will also bring some energy flux to the wall. This heat flux is estimated to be approximately equal to the escaping-electron heat flux. A more exact solution of the full problem is currently being pursued with numerical methods. A full illustration of the electron distribution function, F, is shown in Fig. 6. The main parts of F are the trapped electrons with

$n_e^{trap} \approx 3\ n_o$ and two beams of cold (n_e^{cold}) and escaping (n_e^{hot}) electrons that have approximately the same density, i.e.,

$$n_e^{hot} \approx n_e^{cold} \approx \frac{n_0 r L}{h V_{Te} \tau_p} \approx 10^{-2} n_0 . \qquad (4\text{-}6)$$

Such a situation with two different beams was studied previously [16]. The two-beam distribution is usually unstable and can give rise to two-stream electron instability. Turbulent friction between the beams, as well as between the beams and the main electron population, will result in a decrease in beam velocity and in heating. A full analysis of these instabilities is beyond the scope of this work and requires more detailed investigation.

V. Normal Operation

During normal operation, unlike the disruption case, ion density in the SOL is very low. This is true because the ion time of flight remains roughly the same as during disruption, but particle confinement time in the core plasma is much longer:

$$\tau_p \approx 10\ \tau_E \approx 10\ s, \qquad (5\text{-}1)$$

and $n_i \approx 10^{-3}\ n_o$. Because of this low ion density, the calculated potential is also low:

$$P^* \approx 0.4 \text{ and } \psi_0 \approx 0.2 . \tag{5-2}$$

The above results are obtained assuming that the heat conduction flux from the core plasma to the SOL is negligible. This assumption may be valid during the disruption scenario, but during normal operation–even with enhanced confinement–the conductive heat flux, W_k, can exceed by one order of magnitude the heat flux, W_s, carried by the plasma particles crossing the separatrix:

$$W_s = \frac{3}{2} k T_o S_{in} \cdot \alpha$$
$$S_{in} = \frac{n_o}{\tau_p}, \quad \alpha = \frac{T_s}{T_o} < 1, \tag{5-3}$$

where T_s is the temperature of the plasma crossing the separatrix. The ratio of the conductive heat flux to the particle heat flux, ξ_s, is then given by

$$\xi_S = \frac{W_k}{W_p} = \frac{2}{\alpha} \frac{\tau_p}{\tau_k} . \tag{5-4}$$

To account for the influence of heat conduction, one can assume that the conduction heat flux is distributed among the trapped electrons [8]. This seems reasonable because the lifetime of

the trapped electrons is controlled by Coulomb collisions. Heating of the trapped electrons will result in faster escape of trapped electrons by overcoming the confining potential. Additional heating of the trapped electrons will therefore result in the requirement of a higher stopping potential in order to neutralize the positive ion charge density, which is fixed by the negative charge of the trapped electrons.

To analyze the effect of heat conduction on the trapped electron distribution function, one can modify Eq. 3-8 to consider the incoming electrons as a Maxwellian distribution but with an enhanced temperature by ξ_S times. Using this consideration, one can use all the previously obtained results with the assumption that the ion temperature remains the same. This means that the collision frequency, ν_o, must be reduced by $\xi_S^{3/2}$ times. Therefore, the new parameters are given by

$$
\begin{aligned}
\nu_h &= \nu_o / \xi_S^{3/2} \\
a_h &= a_o \left(\frac{\nu_o}{\nu_h} \right)^{5/11} = a_o \, \xi_S^{15/22} \\
P_h &= P^* \left(\frac{a_o}{a_h} \right)^{1/5} = P^* \, \xi_S^{-3/22} \\
\psi_h &= \psi_o \left(\frac{P_h^*}{P^*} \right) = \psi_o \, \xi_S^{-3/11}.
\end{aligned}
\qquad (5\text{-}5)
$$

From the above equations, the dimensionless potential, ψ^*, is decreased by $\xi_s^{3/11}$ times, but the actual potential is increased:

$$\frac{e\phi_o}{kT_o} = \psi^* \xi_s = \psi_o \xi_s^{8/11}. \tag{5-6}$$

For $\tau_p \approx 10\tau_E$ and, $\alpha = 1$, the value of $\xi_s \approx 20$. Therefore,

$$\frac{e\phi_o}{kT_o} \approx 1.9. \tag{5-7}$$

This value of the wall potential during the enhanced phase of normal operation seems reasonable and is in reasonable agreement with numerical Monte Carlo calculations [8].

In the above analysis, the coefficient of secondary electron emission is assumed equal to 1. This is true for the disruption case since the hot and dense vapor cloud that developed from the wall because of plasma energy deposition has very high emissivity. Lower wall emissivity will increase the stopping potential. The influence of the emissivity on the wall potential in a collisionless SOL, however, was previously shown to be small [8].

The dynamic friction and diffusion coefficients were obtained in Eq. 3-5 with the assumption of a Maxwellian distribution function of the trapped electrons with $T = T_o$. However, it was shown from Eq. 4-1 that the actual temperature (or mean energy) of the trapped electrons is lower than that, i.e., $T_t \le e\phi_o/kT_o \approx 0.5\, T_o$. Because ϕ_o depends only weakly on T_t (ϕ_o

$\propto T^{-3/11}$), the accuracy of these assumptions for this study seems acceptable in order to understand the general dependence of device parameters on a collisionless SOL.

The inclusion of particles in region II (see Fig. 3) should decrease the wall potential due to the increased phase space area of the trapped electrons. This is a result of the additional diffusion time required for the particles to leave region II and escape to the wall. Decreasing of the flux of the trapped electrons, i.e., increasing the escaping flux, will decrease the wall potential, $|\phi|$. Therefore, slightly better confinement of the trapped particles is expected.

No sufficient data are available on the ratio of the thermal and particle fluxes arriving from the core plasma during plasma disruptions. Conventional opinion assumes that the heat flux, $W_k = k\nabla T$, is equal to zero, and this assumption is also used in this study. However, recent data from current tokamak machines such as JET indicate that the thermal phase of a plasma disruption can be divided into two stages [10]. First, there is a slow decrease in T_e during about 70% of the disruption phase, followed by a fast decrease of T_e almost to zero during the remaining part of the thermal phase of disruption. This may suggest that heat conduction during a disruption could play a role in the dynamics of SOL parameters.

IV. Summary

During conventional divertor operations, the plasma in the scrape-off layer (SOL) is highly collisional. However, a new divertor operational scenario with high-temperature, low-density plasma has been proposed to enhance energy confinement in helical devices and in tokamak machines. Therefore, the study of a collisionless high-temperature, low-density SOL plasma becomes important. In addition, the SOL plasma during disruptions in most fusion devices is always shown to be collisionless.

The collisionless SOL plasma during normal operations was recently studied in different fusion devices. The main idea of these studies is that the ions and electrons coming from the core plasma with similar fluxes ($S_i = S_e = S_{in}$) will leave the SOL with different flight times (lifetimes) due to the large differences in their thermal velocities $\left(V_{Te}/V_{Ti} = \sqrt{M/m}\right)$. For charge neutralization, the existence of trapped electrons between the two opposite divertor plates is, therefore required. The fact that a negative potential, ϕ_o, exists between the SOL plasma and the divertor walls (or the vapor cloud near the divertor plates during a disruption) actually means that the SOL is the electrostatic trap for electrons. Ions, in contrast, are accelerated toward the walls.

Electrons arriving at the SOL will face two different fates. Electrons with parallel energy, $E_{\parallel} < e\phi_o$, are trapped and can leave the trap only due to collisions, i.e., diffusion in phase space. The remaining electrons with $E_{\parallel} > e\phi_o$ will quickly escape the SOL in $\tau_{\parallel}^{e}$ time. A cold secondary electron flux is emitted from the walls as a result of the fast-escaping electrons. Therefore, the

problem consists of solving the Fokker-Planck equation for the SOL plasma with source electrons arriving from the core plasma and electron losses at the boundary in phase space ($E_{||} = e\phi_o$).

We have developed an analytical solution that uses a simplified form of the Fokker-Planck equation for a collisionless plasma condition in the SOL. This analytical solution, despite the simplified assumptions, provides a quick and very useful insight into the role of different physical and geometrical processes in the behavior of a collisionless SOL during both plasma disruptions and normal plasma operation of the enhanced phase of high-temperature, low-density plasma. This analytical solution is in good agreement with numerical solutions that use Monte Carlo methods. The developed treatment of the collisionless plasma in this study allows one to avoid artificial assumptions based on the theory of the Langmuir probe used in previous studies of a collisional plasma to study SOL behavior during disruptions.

The main results of this analytical work can be summarized as:

1. Confirmation that the potential between the divertor plates and the SOL of a collisionless plasma is relatively low, i.e., $e\phi/kT < 1$.
2. The ion charge in the SOL is mainly neutralized by the trapped electrons.
3. The dependence of the sheath potential, ϕ, on device parameters is given by

$$\phi \sim \left(\frac{R^2 r}{\tau_p \, h \, T^{5/2}} \right)^{2/11}$$

for a wide range of fusion devices.

4. Electron distribution in the SOL includes four different electron beams (two hot electron beams and two cold electron beams). Existence of such beams can result in two-stream electron instability. The consequence of this turbulent instability is that the SOL plasma can be collisional with the turbulent path length, λ_T, of the electron beams approximately the same length as that of the SOL, i.e., $\lambda_T \approx L$.

The analytical results obtained in this study were made possible only through some simplified assumptions. More detailed considerations and more elaborate solutions that use numerical methods for the nonlinear Fokker-Planck equation are required for a better and more comprehensive understanding of the roles of all physical processes involved. Such a study is currently underway.

Acknowledgments

This work is supported by the U.S. Department of Energy.

References

[1 R. Parker, G. Janeschitz, H. D. Pacher, D. Post, S. Chiocchio, G. Federici, P. Ladd, J. Nuclear Materials, 241-243 (1997) 1.

[2] A. Hassanein, "Response of Materials to High Heat Fluxes during Operation in Fusion Reactors," ASME, 88-WA/NE-2 (1988).

[3] A. Hassanein and I. Konkashbaev, Plasma Devices and Operations, Vol. 5 (1998) 297.

[4] I. K. Konkashbaev, Plasma Phys., Rep. 19 (8), Aug. (1993) 496.

[5] N. Ohyabu, T. Watanabe, H. Ji, H. Akao, *et al.*, Nucl. Fusion 34 (1994) 387.

[6] H. Takase and N. Ohyabu, Nucl. Fusion 35 (1995) 123.

[7] M. Shimada and JT-60 TEAM, 14th Int. Conf. on Plasma Physics and Controlled Nuclear Fusion Research, Wurzburg, Germany, 30 Sept.-7 Oct., 1992, IAEA, Vienna, Vol. 1, p. 57 (1993).

[8] W. X. Wang, M. Okamoto, N. Nakajima, S. Murakami, N. Ohyabu., Nucl. Fusion 37 (1997) 1445.

[9] P. J. Catto and R. D. Hazeltine, Phys. Plasmas 1 (6) (1994) 1882.

[10] D. J. Ward and J. A. Wesson, Nuclear Fusion, Vol. 32. No. 7 (1992) 1117.

[11] V. V. Mirnov, Private Communication, 1997.

[12] D. V. Sivukhin, Reviews of Plasma Physics, Vol. 4, M. A. Leontovich, ed., Consultants Bureau, New York (1966).

[13] N. A. Krall and A. W. Trivelpiece, Principles of Plasma Physics, McGraw-Hill (1968).

[14] M. N. Rozenbluth and R. Z. Sagdeev, Handbook of Plasma Physics, Vol. II, General Editions, North-Holland (1980).

[15] V. P. Pastukhov, Reviews of Plasma Physics, Vol. 13, B. B. Kadomtsev, ed., Consultants Bureau, New York-London (1987).

[16] I. K. Konkashbaev and A. P. Ponomarev, Sov. Plasma Physics, Vol. 16 No. 1 (1990) 3.

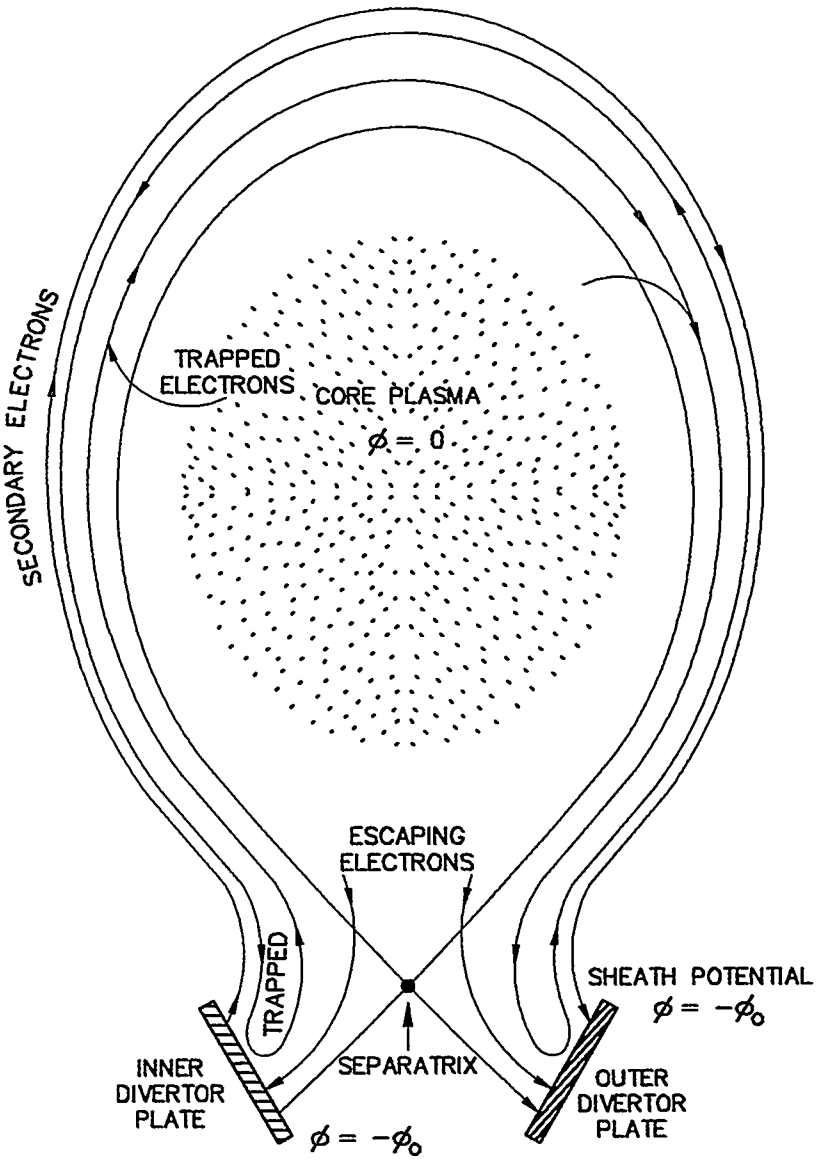

Fig.1 Schematic illustration of electron population in a collisionless SOL between inner and outer divertor plates in a tokamak device

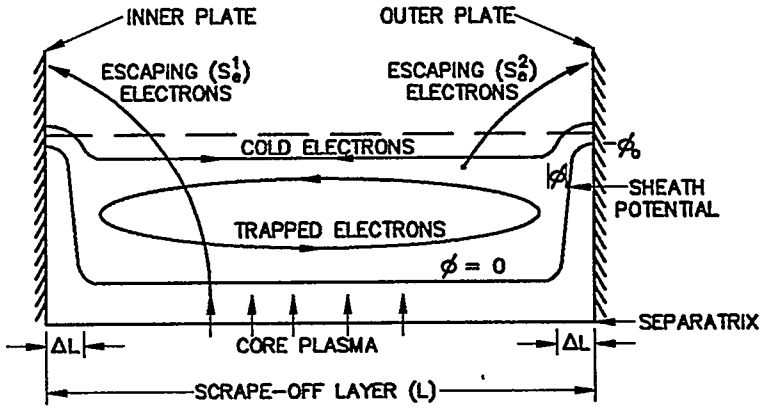

Fig.2 Schematic view of different electron populations in SOL described in the used model

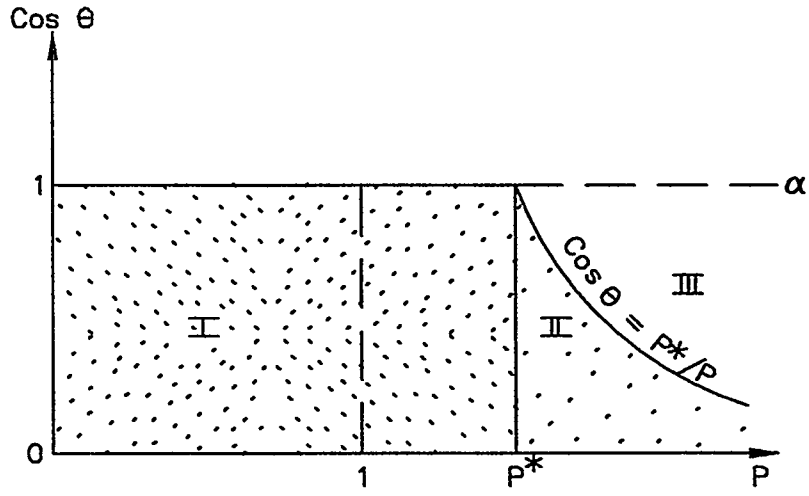

Fig.3 Regions of trapped electrons in momentum space

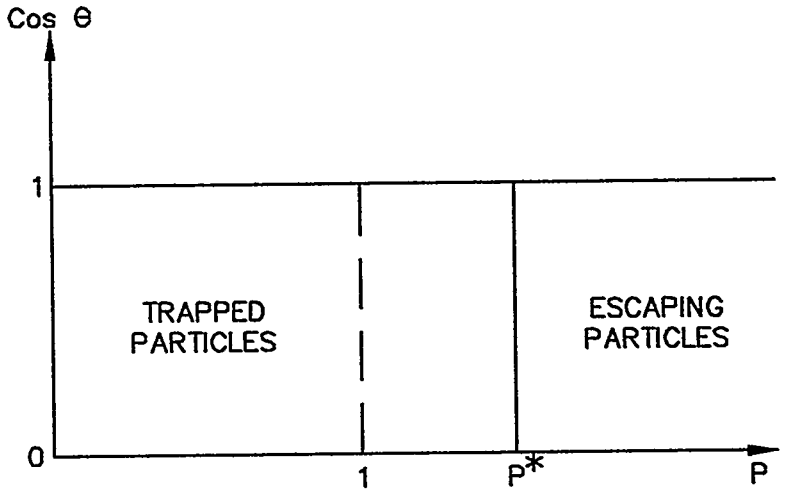

Fig.4 Trapped electrons in momentum space for reduced problem

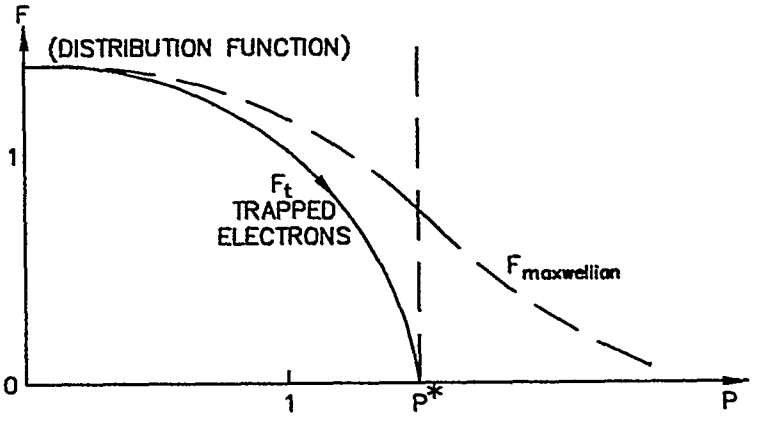

Fig.5 Distribution function of trapped electrons in SOL, compared to a Maxwellian distribution function

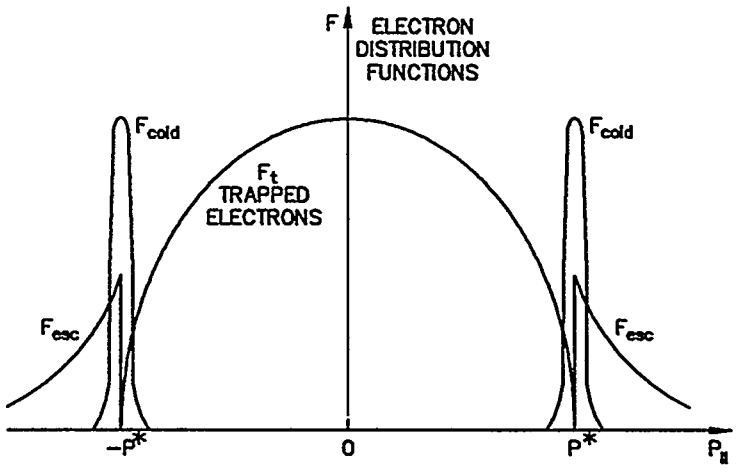

Fig.6 Distribution functions of three different electron populations in SOL

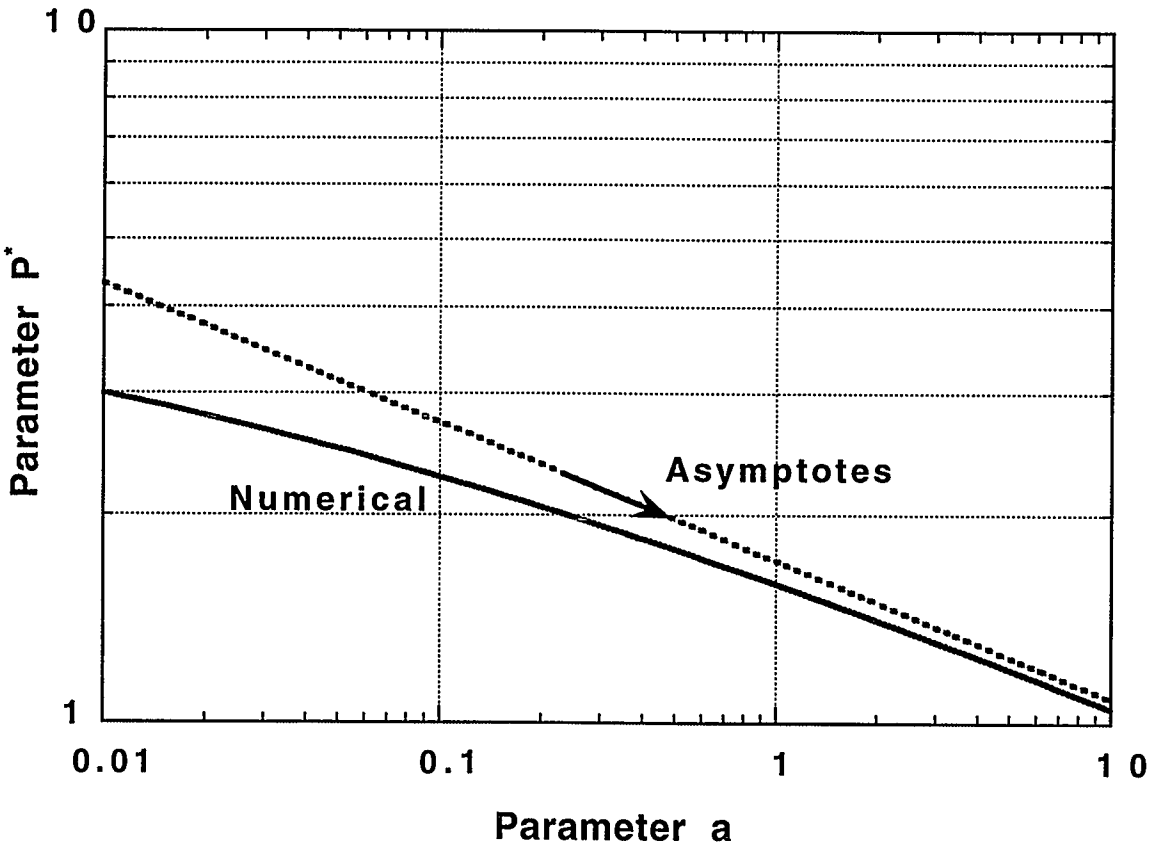

Fig. 7 Dependence of boundary momentum P on the tokamak parameter a.

DISTRIBUTION LIST FOR ANL/FPP/TM-296

Internal

S. Bhattacharyya
J. Brooks
Y. Chang
D. Diercks
D. Ehst
Y. Gohar
D. Gruen
A. Hassanein (5)
R. Mattas
R. Poeppel
W. Shack
D. L. Smith
R. Valentin
R. W. Weeks
FPP Files (15)
TIS File

External

ANL-E Library
ANL-W Library
DOE/OSTI, for distribution (2)
M. Akiba, Japan Atomic Energy Research Institute, Japan
C. Baker, University of California, San Diego
C. Bathke, Los Alamos National Laboratory
S. Berk, U.S. Department of Energy
H. Bolt, Institute for Materials in Energy Systems – IWE, Germany
C. Bolton, U.S. Department of Energy
R. Causey, Sandia National Laboratories, Livermore
R. Conn, University of California, San Diego
R. Dagazian, U.S. Department of Energy
W. Dove, U.S. Department of Energy
L. El-Guebaly, University of Wisconsin
G. Emmert, University of Wisconsin
N. J. Fisch, Princeton Plasma Physics Laboratory
R. Goldston, Princeton Plasma Physics Laboratory
S. Jardin, Princeton Plasma Physics Laboratory
C. E. Kessel, Princeton Plasma Physics Laboratory
V. Kozherin, Ioffe Institute, St. Petersburg, Russia
Y. Martynenko, Kurchatov Institute, Russia
D. Mikkelsen, Princeton Plasma Physics Laboratory
F. Najmabadi, University of California, San Diego
W. Nevins, Lawrence Livermore National Laboratory
H. Nickel, Institute for Materials in Energy Systems – IWE, Germany
R. Nygren, Sandia Natiional Laboratory
A. Opdenaker, U.S. Department of Energy
J. Perkins, Lawrence Livermore National Laboratory
N. Sautoff, Princeton Plasma Physics Laboratory
M. Sawan, University of Wisconsin
M. Seki, Japan Atomic Energy Research Institute, Japan
W.M. Stacey, Georgia Institute of Technology
D. Steiner, Rensselaer Polytechnic Institute
I.Sviatoslavsky, University of Wisconsin

M.Ulrickson, Sandia National Laboratory, Albuquerque, NM
J. Van der Laan, ECN, Netherlands
J. Vetter, Forschungszentrum Karlsruhe, Germany
G. Vieider, ITER, Germany
F.W. Wiffen, U.S. Department of Energy
K. Wilson, Sandia National Laboratories, Livermore
Bibliothek, Max-Planck-Institute fur Plasmaphysik, Germany
C.E.A. Library, Fontenay-aux-Roses, France
Librarian, Culham Laboratory, England
Thermonuclear Library, Japan Atomic Energy Research Institute, Japan